VELOCITY ANALYSIS ON CMP SECTIONS BASED ON THE SMEARING PARADIGM

D.L. Macedo, J.J.S. Figueiredo, R.S. Portugal, and J. Schleicher

email: *dlmacbr@gmail.com*

keywords: *Velocity analysis, CMP techniques, smearing*

ABSTRACT

The construction of coherence panels in the velocity spectrum is traditionally achieved by summing up amplitudes along auxiliary hyperbolae that are parameterised by zero-offset time and stacking velocity, using semblance as the coherency measure. In this work we investigate how some of these methods could benefit of smearing instead of stacking procedures. We implement and compare two smearing methodologies – smearing the total amplitude, and smearing with constant amplitude density. We show that smearing the total amplitude leads to semblance as coherency measurement, thus recovering conventional velocity spectra. Thus, using the smearing procedure may be an advantageous alternative to using the stacking paradigm, especially because of its potential for parallel computing. Using the amplitude density gives rise to a slightly different coherency measure, which we call semblance-like. Our numerical experiments indicate that this measure might be able to improve the focussing of the velocity peaks in the velocity spectra.

INTRODUCTION

CMP-based techniques, such as NMO correction, stacking and velocity analysis, are considered the core of seismic processing, mainly because their products will feed more advanced and critical procedures, such as migration and inversion. As a matter of fact, errors during the early stages of seismic processing often accumulate, generating mispositioned reflectors and bad geologic interpretation.

All these techniques have in common that, in general, they are all theoretically based on velocity model assumptions, associated to a traveltime expression, which is obtained from a combination of procedures that relies on the physics of waves and geometrical optics. The design of the actual technique from the theoretical model employs numerical schemes that are based on signal processing, basic laws of statistics and numerical analysis. For instance, the simplest form of velocity analysis is based on a layered geological model, in which the layers are homogeneous and separated by horizontal flat interfaces. The associated traveltime expression is the hyperbolic traveltime formula, which depends of the offset and is parameterised by RMS velocity and zero-offset traveltime, both obtained from the model (Dix, 1955; Castle, 1994). Also, the numerical scheme is based on the semblance formula, which is, roughly speaking, a quotient between the squared sum of amplitudes and sum of squared amplitudes collected along hyperbolic curves (Taner and Koehler, 1969).

Although velocity analysis using CMP sections and coherency measurements is already a well established procedure in practice, it has been subject to further theoretical studies since its formal introduction by Taner and Koehler (1969). Many modifications and extensions to the original idea have been proposed, all of them improving or changing the geologic model and/or the coherency measurements. Concerning improvements related to the geologic model or traveltime expression there is, for instance, the inclusion of anisotropy factors (Alkhalifah and Tsvankin, 1995), the geometrical correction of traveltime curves (de Bazelaire, 1988) or considering non hyperbolic curves (Abbad et al., 2009). On the other hand, concerning the improvements that address coherence measurements, we can cite, for example, the improvement of

statistical measurements of coherence (Neidell and Taner, 1971) and the introduction of differential semblance (Li and Symes, 2007). Common to all of these modifications is the basic principle, i.e., the stacking neighbouring traces to detect a best possible stacking velocity.

There is another set of procedures in the seismic method that relies on stacking. A great many of imaging processes has its theoretical basis in integrals computed along auxiliary curves, such as Kirchhoff migration (Hubral et al., 1996; Tygel et al., 1996) or tau-p transforms (Clayton and McMechan, 1981). Actually these integrals explain theoretically why stacking amplitudes along auxiliary curves gives goods results. Also, we can understand stacking amplitudes as the direct translation of theoretical formulas to practical problems, with the only difference that the integral operation changes into a discrete summation.

The usual methods of velocity analysis, as well as its variants and extensions, are all designed under the same principle, which is generically referred to as stacking, and which can be divided in three parts:

Location Consider a traveltime function which is geometrically equivalent to a line (or surface).

Measurement Design some statistical measurement that gives some desired property, such as coherency.

Stacking On the intersection of *Location* and the data section, apply the *Measurement*.

Therefore, by the term "stacking", we mean to perform the numerical computation using the data collected along a curve defined by the traveltime expression. For instance, the construction of coherency panels in a velocity spectrum (VS) are usually made by properly summing up amplitudes and squared amplitudes along auxiliary hyperbolae, which are parameterised by zero-offset time t_0 and stacking velocity v.

As is well-known in seismic imaging, Kirchhoff-type operations can be as well realized as a stacking as a smearing process. Both are described by the same theoretical integrals and differ from each other only by the order of the nested loops and possibly necessary interpolations. In complete analogy, we propose in this work a change of paradigm for the construction of velocity spectra, i.e., to perform velocity analysis on coherency panels constructed by *smearing* instead of stacking.

In the case of seismic migration, the smearing paradigm means that the amplitudes of seismic traces are smeared along isochrons in the migrated image (Santos et al., 2000). Actually, Kirchhoff migration by smearing can be seem as a memory saving way to perform migration on massively pre-stack data, because each trace can be used independently, pointing towards its potential for parallel algorithms.

When applying the smearing paradigm to the construction of velocity spectra, we use the conventional geological model and traveltime expression, i.e., we consider a RMS velocity model and the hyperbolic traveltime expression. Also, as coherency measurement we choose the semblance as a starting formula. The main difference is that the CMP data are no longer summed for a single point of the velocity spectrum along a hyperbola in the CMP gather to produce the corresponding semblance value, but the amplitude of each sample of CMP section is spread along a proper curve that lies on the velocity spectrum.

Two steps must be taken to develop the proposed method:

- Define smearing curve expression;
- define the method to evaluate the semblance measurement in the smearing process.

These items are discussed in the following sections.

FAMILY OF HYPERBOLAE

In order to build the smearing curve corresponding to a single point in CMP section, we start by considering a family of hyperbolae which pass through this point. The well-known basic formula of the hyperbolic traveltime is

$$t^2 = t_0^2 + (x/v)^2 \,, \tag{1}$$

where t is the reflection time, t_0 is the zero-offset (ZO) time, x is the offset and v is the medium velocity or RMS velocity of the above layers. The above formula tells us that for each (v, t_0) pair in the velocity spectrum, there is a hyperbola in the CMP gather and vice-versa. Conventional velocity spectra are constructed by summing the CMP data along curves (1) for a set of values for t_0 and v.

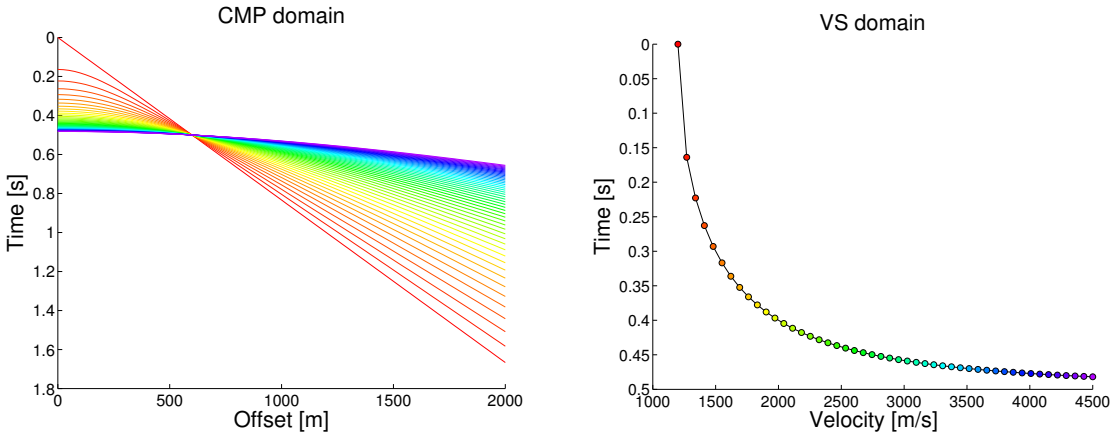

(a) CMP gather. **(b)** Velocity spectrum.

Figure 1: A family of hyperbolae depicted in (a) intersect at one given point in the CMP gather. Each hyperbola in the CMP gather depicted in (a) can be associated to a single point in the velocity spectrum (b), represented by a circle with the same colour.

To develop our approach, we seek a family of hyperbolae which intersection is at a given point (x_i, t_i). In this way, we simply require that the parameters t_0 and v must satisfy

$$t_i^2 = t_0^2 + (x_i/v)^2 \,. \tag{2}$$

Isolating t_0 we obtain a relationship

$$t_0^2 = t_i^2 - (x_i/v)^2 \,, \tag{3}$$

where we require that $v \geq x_i/t_i$ to guarantee that $t_0 \geq 0$. Inserting equation (3) in (1), we obtain a general equation

$$t^2 = t_i^2 - (x_i/v)^2 + (x/v)^2 \,, \tag{4}$$

which represents a family of hyperbolae that intersect at (x_i, t_i), in which v is the family parameter. Figure 1(a) shows a family of hyperbola intersecting one point.

Each single hyperbola of the family of intersecting hyperbolae corresponds to a point (v, t_0) in the velocity spectrum to be constructed. Therefore, the whole family of hyperbolae described by equation (4) corresponds to a curve in the velocity spectrum given by

$$t_0 = f(v) = \sqrt{t_i^2 - (x_i/v)^2} \,, \tag{5}$$

where v must be greater than x_i/t_i. Figure 1(b) shows the line that represents the family of hyperbolae depicted in Figure 1(a). Notice that each coloured hyperbola shown in Figure 1(a) has a one-to-one correspondence to a point, depicted as circle of the same colour in Figure 1(b).

Therefore, for each point (x_i, t_i) in the CMP gather, we can establish an one-to-one relationship to a curve Γ_i in the velocity spectrum, i.e.,

$$(x_i, t_i) \longleftrightarrow \Gamma_i \,,$$

where Γ_i is defined as

$$\Gamma_i \;=\; \left\{ (v, t_0) \mid t_0(v) = \sqrt{t_i^2 - (x_i/v)^2}, \quad v \geq x_i/t_i \right\}. \tag{6}$$

Note that the smearing curve is a hyperbola as well.

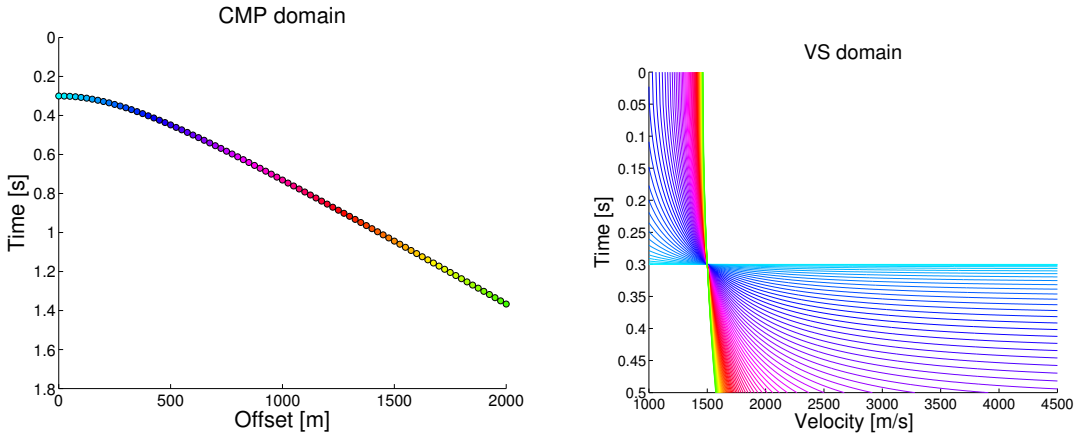

(a) CMP gather. **(b)** Velocity spectrum.

Figure 2: (a) Reflection event hyperbola in the CMP gather. (b) Smearing curves in the velocity spectrum. Each hyperbola in the velocity spectrum is associated with a point in the CMP gather (circle in the same colour).

COHERENCY PANEL BY SMEARING

The basic idea behind building up coherency panels by smearing is shown in Figure 2. In Figure 2(a), there is a hyperbola representing a reflection event, with RMS velocity v and ZO time t_0. Also shown is a smearing curve associated with each picked point along the event in the CMP gather, according to equation (6). Note that these curves intersect exactly at point (v, t_0) in the velocity spectrum, as seen in Figure 2(b). It is this property that makes the construction of the coherency panel by smearing possible.

To construct a velocity spectrum by smearing we need to distribute the energy found in a CMP gather at a point (x_i, t_i) along the associated hyperbola. Below, we compare two methods of distributing this energy:

Smearing total amplitude In this method, all points of the velocity spectrum that lie on the smearing curve receive exactly the amplitude value from the corresponding CMP gather point (x_i, t_i).

Smearing by constant amplitude density In this procedure, the points that lie on the smearing curve receive values associated with the amplitude density at point (x_i, t_i). This amplitude density is defined as a constant fractional part of the total amplitude at the corresponding CMP domain point (x_i, t_i) such that the integration (summation) along the distribution curve recovers the original amplitude. In other words, the amplitude density is the amplitude value at (x_i, t_i) divided by the length of the smearing curve.

It must be kept in mind that the smearing is carried out in a discretised domain, i.e., the velocity spectrum to be constructed is defined on a grid. Therefore, throughout the smearing process, values need to be assigned to points on the grid. Hardly ever, the smearing curve will actually pass through a grid point. This implies that some kind of interpolation rule must be established to attribute amplitude values to the points in the close vicinity to the smearing curve as well. In the following, we will say that all points in this vicinity that effectively receive amplitude information in the smearing process *lie on the smearing curve*.

In a conventional velocity spectrum, the coherency measure is usually semblance, which is mathematically expressed as (Taner and Koehler, 1969)

$$S(v_{NMO}, t_0) = \frac{\sum_{\Delta} \left[\sum_{i=1}^{m} f_i(t_i + \Delta) \right]^2}{m \sum_{\Delta} \sum_{i=1}^{m} f_i^2(t_i + \Delta)} . \tag{7}$$

Here, m is the number of traces in the CMP domain, and $f_i(t_i)$ is the amplitude at time t_i of the trace f_i at x_i. Time t_i is the hyperbolic traveltime defined as

$$t_i = \sqrt{t_0^2 + \frac{x_i^2}{v_{NMO}^2}}, \tag{8}$$

where v_{NMO} is the trial NMO velocity. Finally, the sum over Δ represents a sum over a time window around time t_i.

Frequently, velocity spectra are built using a simpler simpler version of semblance that does not use the time-window sum. In this case, equation (8) reduces to

$$S'(v_{NMO}, t_0) = \frac{\left[\sum_{i=1}^{m} f_i(t_i)\right]^2}{m \sum_{i=1}^{m} f_i^2(t_i)}. \tag{9}$$

In the smearing process, both types of coherency measures can be obtained, too. For this purpose, it suffices to to smear the amplitude, $f_i(t_i)$, and the squared amplitude, $f_i^2(t_i)$, into separate panels and then divide the resulting "partial" panels point by point to obtain the "final" panel. Below we discuss the details of this procedure for the two types of amplitude values to be used in the smearing.

Smearing total amplitude

To build up the final panel in this method, we actually need three partial panels:

Panel A This panel is the result of the amplitude $f_i(t)$ smearing. It will be squared, point-by-point, after the smearing process.

Panel A2 This panel results from the smearing process of the squared amplitudes $f_i^2(t)$.

Panel M The third panel keeps track of the number of times some value is assigned to each point (v, t_0) in the panels A and A2.

The final panel *S'* can then be built from the three partial panels described above using the point-by-point operation

$$S' = \frac{[A]^2}{M\,A2}. \tag{10}$$

Done in this way, the process leads to the build up of the unwindowed semblance as defined in equation (9) as the desired coherency measure at each output point in the velocity spectrum. An example can be seen in Figure 3.

To see that the result of the above procedure leads to the unwindowed semblance, consider a point Q with coordinates (v_Q, t_{0Q}) in the velocity spectrum to be constructed. Since there are m traces in the CMP gather, there are m smearing curves that pass through Q. In the first smearing process (panel A), each one of these curves deposits in Q the values $f_i(t_i)$ that correspond to each one of the points over a possible reflection event on CMP domain. After smearing these m events, the sum at Q in panel A will have received

$$A(v_Q, t_{0Q}) = \sum_{i=1}^{m} f_i(t_i). \tag{11}$$

The panel A2 is constructed by a corresponding process with the squared amplitudes, $f_i^2(t_i)$. Thus, the value found in Q after smearing the m amplitude squares is

$$A2(v_Q, t_{0Q}) = \sum_{i=1}^{m} f_i^2(t_i). \tag{12}$$

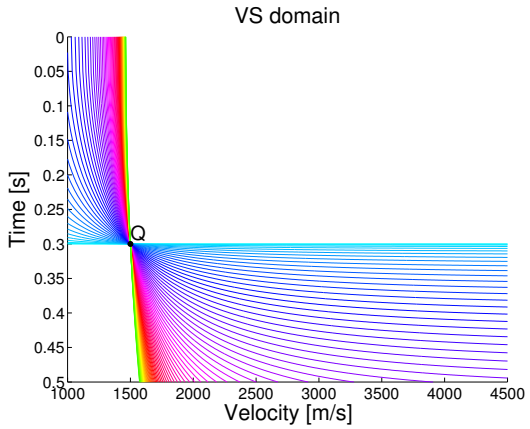

Figure 3: A point Q in the velocity spectrum through which smearing curves pass that correspond to points in the CMP gather on a possible reflection event.

As long as m smearing curves pass through Q, one finds that $M(v_Q, t_{0Q}) = m$. Therefore, the final panel S' will receive the value

$$S'(v_Q, t_{0Q}) = \frac{[A(v_Q, t_{0Q})]^2}{M(v_Q, t_{0Q})\, A2(v_Q, t_{0Q})} = \frac{\left[\sum_{i=1}^{m} f_i(t_i)\right]^2}{m \sum_{i=1}^{m} f_i^2(t_i)}. \tag{13}$$

The count m may be smaller at points close to the border of the velocity spectrum, where less than m hyperbolae may pass through the selected point Q.

Smearing by constant amplitude density

When smearing the constant amplitude density, only two partial panels are needed to build up the final panel:

Painel A' Similar to Panel A before, this panel is the result of the amplitude density $d_i(t)$ smearing. It will be squared, point-by-point, after the smearing process.

Panel A2' Similar to Panel A2 before, this panel results from smearing the squared amplitude densities $d_i^2(t)$.

The amplitude-density smearing does not need a Panel M that counts the number of hits for the calculation of the semblance.

The final panel *Sl* is then built up by the point-by-point operation

$$Sl(v, t_0) = \frac{[A'(v, t_0)]^2}{A2'(v, t_0)}. \tag{14}$$

However, smearing out the constant amplitude density actually does not lead to semblance as the coherency measure. It rather produces a similar value slightly different from semblance. Let us follow the procedure step by step as before to find the coherency measure determined by this procedure. We again consider a point Q in the velocity spectrum to be constructed (see again Figure 3). After the smearing process in the first partial panel A', we get at Q

$$A'(v_Q, t_{0Q}) = \sum_{i=1}^{m} \frac{f_i(t_i)}{s(x_i, t_i)} \Delta s(x_i, t_i), \tag{15}$$

in which $\Delta s(x_i, t_i)$ is the smearing curve's local length at Q. Here, the smearing curve's local length is its length within the current grid cell that contains point Q. Variable $s(x_i, t_i)$ denotes the smearing curve's total length within the velocity spectrum. In this way, $d(x_i, t_i) = f_i(t_i)/s(x_i, t_i)$ is the amplitude density associated with the input point (x_i, t_i).

The panel A2' resulting from the smearing process of the squared amplitude, gives, in point Q, the value

$$A2'(v_Q, t_{0Q}) = \sum_{i=1}^{m} \frac{f_i^2(t_i)}{s(h_i, t_i)} \Delta s(x_i, t_i). \tag{16}$$

The final panel *Sl*, built up by point-by-point operation $Sl = (A')^2/A2'$, gives in the same point Q the value

$$Sl(v_Q, t_{0Q}) = \frac{\left[\sum_{i=1}^{M} \frac{f_i(t_i)}{s(x_i, t_i)} \Delta s(x_i, t_i)\right]^2}{\sum_{i=1}^{M} \frac{f_i^2(t_i)}{s(x_i, t_i)} \Delta s(x_i, t_i)}. \tag{17}$$

Operation (17) does not need the hit count to produce a semblance-like coherence measure, because the normalisation with the local length of the smearing curve substitutes the normalisation with the hit count.

In order to better understand expression (17), let us make some approximations. Firstly, let us consider the local length $\Delta s(x_i, t_i)$ constant and equal to some mean value $\overline{\Delta s}(v, t_0)$ for all the smearing curves that pass through point Q. This assumption is justified if we consider the grid cell rather small in comparison to the smearing curve's total length. This approximation leads to

$$Sl(v_Q, t_{0Q}) \approx \frac{\left[\sum_{i=1}^{m} \frac{f_i(t_i)}{s(x_i, t_i)}\right]^2 \overline{\Delta s}}{\sum_{i=1}^{m} \frac{f_i^2(t_i)}{s(x_i, t_i)}}. \tag{18}$$

The second approximation concerns the smearing curves' total lengths themselves. Figure 4 shows, in the CMP gather, the smearing curve's lengths that correspond to each point (x, t). This CMP gather shows the same time and offset intervals used in the test model, which will be described later. There are level curves that indicate different smearing curves with the same length. The level curves' trend follows, roughly, the one of the hyperbolic traveltimes. This suggests that the smearing curves' lengths along a typical reflection event may not vary too much, which leads to the second approximation. Let us consider the lengths $s(x_i, t_i)$ constant and equal to some mean value $\bar{s}(v, t_0)$. With this approximation, equation (18) reduces to

$$Sl(v_Q, t_{0Q}) \approx \frac{\left[\sum_{i=1}^{m} f_i(t_i)\right]^2}{\left(\bar{s}/\overline{\Delta s}\right) \sum_{i=1}^{M} \left[u(h_i, t_i)\right]^2}. \tag{19}$$

From expression (19), it is easily recognised that Sl behaves similar to conventional semblance, with the ratio $\left(\bar{s}/\overline{\Delta s}\right)$ replacing the hit count m. For this reason, we will refer to this coherency measure as *semblance-like*.

NUMERICAL EXAMPLES

To prove the concept of the construction of velocity spectra by smearing and to compare the coherency measures discussed above, we tested the technique with synthetic data generated from a simple horizontally-layered model with constant layer velocities. The model description is given below:

1. Four reflectors;

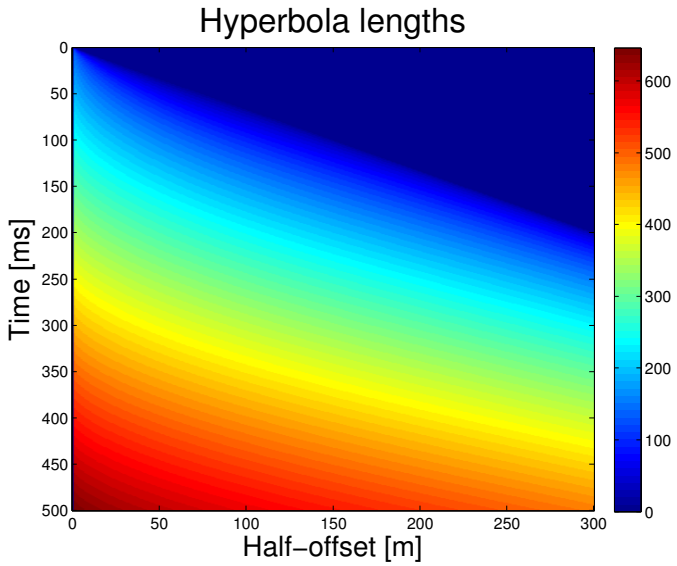

Figure 4: To each point of the CMP domain is assigned the corresponding smearing curve's length in the velocity spectrum. This CMP gather shows the same time and offset intervals used in the test model, which will be described later.

2. layer velocities equal to 1.5 km/s, 2.25 km/s, 2.55 km/s and 3.45 km/s from top to bottom;

3. reflector distances, in units of time, equal to 75 ms, 45 ms, 150 ms and 150 ms from top to bottom;

4. half-offset ranges from 0 m to 300 m, in 1 m steps;

5. time ranges from 0 m to 500 ms, in 1 ms steps;

6. geometric spreading and complex reflection coefficients are not taken into account;

7. random noise added (SNR = 0.332 dB).

The data were modelled using ray tracing in the RMS velocity model. The synthetic data after addition of noise are shown in Figure 5.

The next set of figures exemplify the construction process of the velocity spectra.

Figure 6 shows the three partial panels, *A*, *A2*, and *M*, and the final panel *S'*, resulting from the total amplitude smearing process. The theoretical RMS velocities are displayed as little white circles in the last panel. Note the perfect coincidence of the coherence peaks in the velocity spectrum with the theoretical RMS velocities (red crosses in the last panel).

Figure 7 shows the two partial panels, *A'* and *A2'*, and the final panel *Sl*, resulting from constant amplitude density smearing. We note again the perfect coincidence of the coherence peaks in the velocity spectrum with the theoretical RMS velocities (white circles in the last panel).

In order to permit a comparison between the proposed smearing methods and the conventional stacking technique, we also performed a velocity analysis based on the stacking paradigm with the same synthetic data. In Figure 8, the final panels *Sl*, *S'* and *C* can be seen. The last one is the result of the stacking process. The good coincidence between the theoretical RMS velocities and the coherence peak can also be observed in the conventional stacked velocity spectrum of Panel C. While the semblance result from smearing total amplitudes looks practically identical to that from stacking, we notice that the coherency peaks are more prominent in the semblance-like coherency measure. This points towards its potential of simplifying automatic detection of coherency peaks.

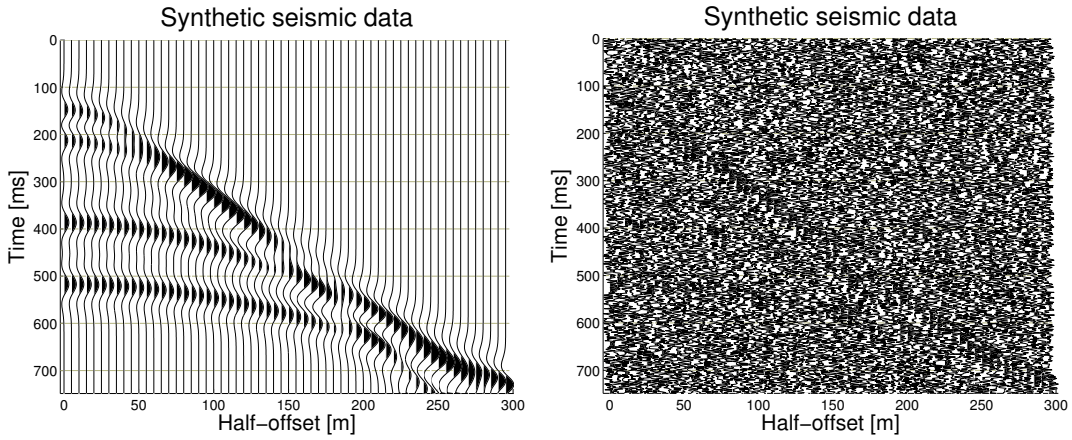

(a) Noise-free data.

(b) Data with noise.

Figure 5: Synthetic data (a) without and (b) with noise, used in the velocity analysis based in the smearing paradigm.

CONCLUSIONS

We have demonstrated that velocity spectra can be constructed with a smearing procedure instead of stacking. For the smearing process, we have compared two slightly different methods that smear the total amplitude or the amplitude density along the smearing hyperbolae. The first observation is that in both smearing methods, the coherency peaks agreed very well with the theoretical RMS velocities, proving the feasibility of the smearing paradigm.

By design, the smearing of the total amplitude leads to a semblance section that is completely equivalent to the velocity spectrum obtained by the conventional stacking procedure. Our numerical test confirmed the expected behaviour. An advantage of the smearing process over stacking is that it can be more easily parallelised, since its acts on one trace at a time. Thus, it should be much faster on parallel computers to construct velocity spectra by smearing than by stacking.

By smearing amplitude densities instead of total amplitudes, we constructed similar velocity spectra, where the coherency measure in this case is a semblance-like function rather than conventional semblance. The coincidence of the coherency peaks with the theoretical RMS velocities was as perfect as for the amplitude smearing. Our numerical experiment indicated that the coherency peaks are easier identified than in conventional semblance panels, particularly with respect to shallow events. This property may warrant its use in spite of its slightly elevated computational cost in comparison to amplitude smearing. Further studies will have to show how the smearing techniques perform in more complicated geological settings and how they react to perturbing influences like stronger noise levels, the presence of coherent noise like multiples, or varying amplitudes along the events.

ACKNOWLEDGEMENTS

This work was kindly supported by the sponsors of the *Wave Inversion Technology (WIT) Consortium*. We also would like to thank the Brazilian research agencies CNPq and CAPES for the scholarships.

REFERENCES

Abbad, B., Ursin, B., and Rappin, D. (2009). Automatic nonhyperbolic velocity analysis. *Geophysics*, 74:U1–U12.

Alkhalifah, T. and Tsvankin, I. (1995). Velocity analysis for transversely isotropic media. *Geophysics*, 60:1550–1566.

Castle, R. J. (1994). A theory of normal moveout. *Geophysics*, 59(6):983–999.

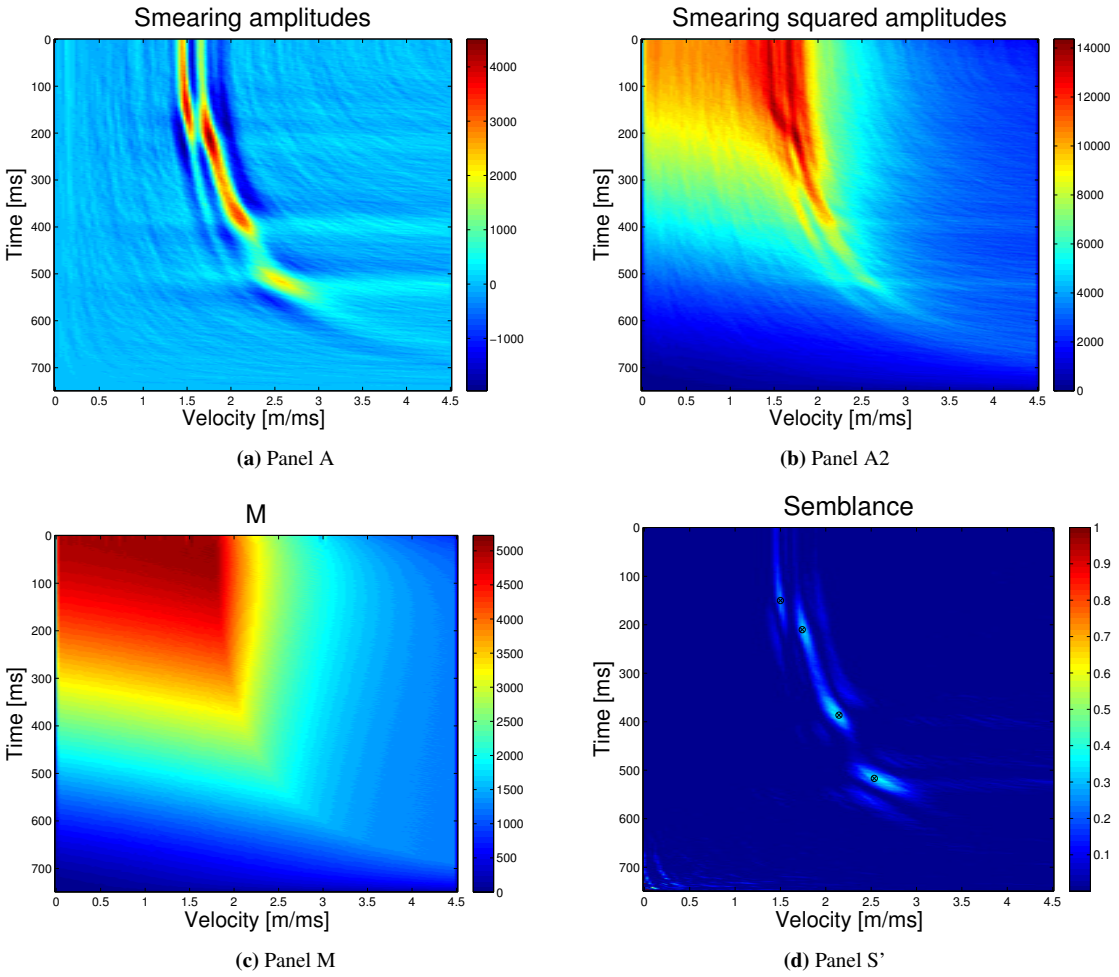

(a) Panel A

(b) Panel A2

(c) Panel M

(d) Panel S'

Figure 6: Results of total amplitude smearing. Also shown in the last panel are the true RMS velocities (red crosses).

Clayton, R. W. and McMechan, G. A. (1981). Inversion of refraction data by wave field continuation. *Geophysics*, 46:860–868.

de Bazelaire, E. (1988). Normal moveout revisited: Inhomogeneous media and curved interfaces. *Geophysics*, 53(2):143–157.

Dix, C. H. (1955). Seismic velocities from surface measurements. *Geophysics*, 20(1):68–86.

Hubral, P., Schleicher, J., and Tygel, M. (1996). A unified approach to 3-D seismic reflection imaging, Part I: Basic concepts. *Geophysics*, 61(3):742–758.

Li, J. and Symes, W. W. (2007). Interval velocity estimation via nmo-based differential semblance. *Geophysics*, 72:U75–U88.

Neidell, N. S. and Taner, M. T. (1971). Semblance and other coherency measures for multichannel data. *Geophysics*, 36(3):482–497.

Santos, L. T., Schleicher, J., Tygel, M., and Hubral, P. (2000). Modeling, migration, and demigration. *The Leading Edge*, 19:712–715.

Taner, M. T. and Koehler, F. (1969). Velocity spectra – digital computer derivation and applications of velocity functions. *Geophysics*, 34(6):859–881.

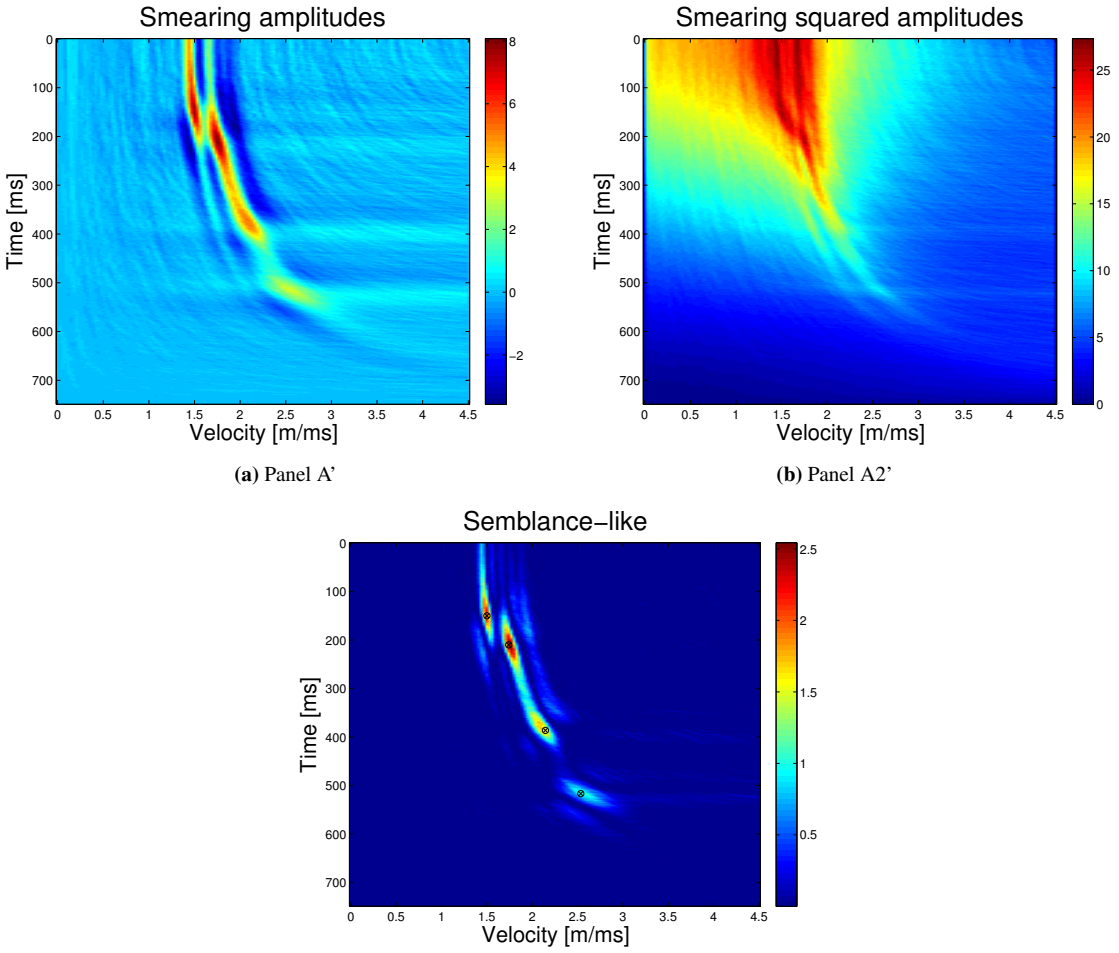

(a) Panel A'

(b) Panel A2'

(c) Panel Sl

Figure 7: Results of constant amplitude density smearing. Also shown in the last panel are the true RMS velocities (white circles).

Tygel, M., Schleicher, J., and Hubral, P. (1996). A unified approach to 3-D seismic reflection imaging, Part II: Theory. *Geophysics*, 61(3):759–775.

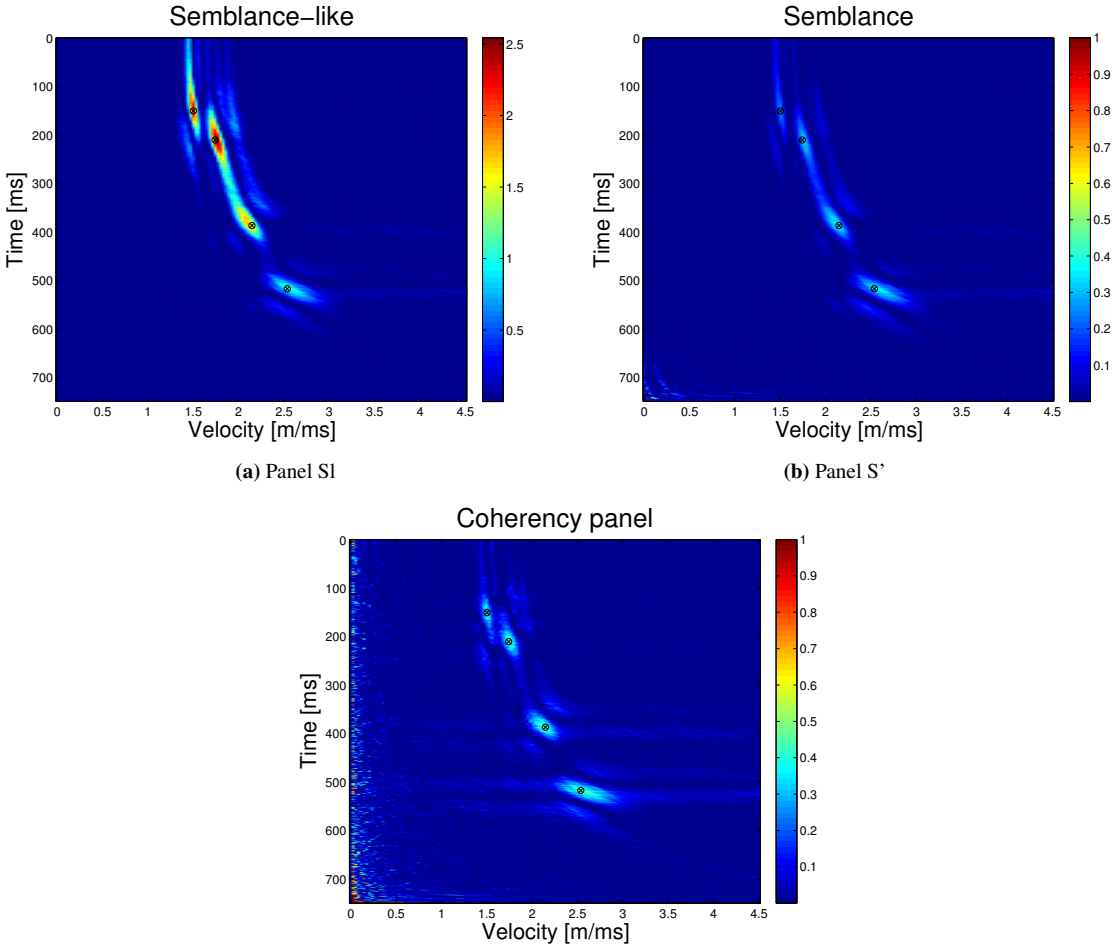

(a) Panel Sl

(b) Panel S'

(c) Panel C

Figure 8: Final velocity spectra constructed by (a) smearing constant amplitude density, (b) smearing total amplitude, and (c) conventional stacking in the CMP gather.